Genome-Wide Identification of the LexA-Mediated DNA Damage Response in *Streptomyces venezuelae*

Kathryn J. Stratton,[a] Matthew J. Bush,[a] Govind Chandra,[a] Clare E. M. Stevenson,[b] Kim C. Findlay,[c] Susan Schlimpert[a]

[a]Department of Molecular Microbiology, John Innes Centre, Norwich Research Park, Norwich, United Kingdom
[b]Department of Biochemistry and Metabolism, John Innes Centre, Norwich Research Park, Norwich, United Kingdom
[c]Department of Cell and Developmental Biology, John Innes Centre, Norwich Research Park, Norwich, United Kingdom

ABSTRACT DNA damage triggers a widely conserved stress response in bacteria called the SOS response, which involves two key regulators, the activator RecA and the transcriptional repressor LexA. Despite the wide conservation of the SOS response, the number of genes controlled by LexA varies considerably between different organisms. The filamentous soil-dwelling bacteria of the genus *Streptomyces* contain LexA and RecA homologs, but their roles in *Streptomyces* have not been systematically studied. Here, we demonstrate that RecA and LexA are required for the survival of *Streptomyces venezuelae* during DNA-damaging conditions and for normal development during unperturbed growth. Monitoring the activity of a fluorescent *recA* promoter fusion and LexA protein levels revealed that the activation of the SOS response is delayed in *S. venezuelae*. By combining global transcriptional profiling and chromatin immunoprecipitation sequencing (ChIP-seq) analysis, we determined the LexA regulon and defined the core set of DNA damage repair genes that are expressed in response to treatment with the DNA-alkylating agent mitomycin C. Our results show that DNA damage-induced degradation of LexA results in the differential regulation of LexA target genes. Using surface plasmon resonance, we further confirmed the LexA DNA binding motif (SOS box) and demonstrated that LexA displays tight but distinct binding affinities to its target promoters, indicating a graded response to DNA damage.

IMPORTANCE The transcriptional regulator LexA functions as a repressor of the bacterial SOS response, which is induced under DNA-damaging conditions. This results in the expression of genes important for survival and adaptation. Here, we report the regulatory network controlled by LexA in the filamentous antibiotic-producing *Streptomyces* bacteria and establish the existence of the SOS response in *Streptomyces*. Collectively, our work reveals significant insights into the DNA damage response in *Streptomyces* that will promote further studies to understand how these important bacteria adapt to their environment.

KEYWORDS *Streptomyces*, DNA damage, SOS response, LexA, RecA

Exposure to genotoxic agents can cause DNA damage with potentially lethal consequences, and therefore the ability to restore genome integrity is an essential task for all living organisms. In bacteria, DNA damage triggers a widely conserved cellular stress response called the SOS response (1). The SOS response is regulated by two key proteins, the activator RecA (a multifunctional recombinase) and the transcriptional repressor LexA. During unperturbed growth, LexA binds as a dimer to a 16-bp palindromic sequence motif, the SOS box, located in the promoter region of its target genes, thereby preventing their expression. Elevated levels of DNA damage can lead to the accumulation of single-stranded DNA (ssDNA), which is sensed and bound by RecA, resulting in the formation of a nucleoprotein filament. This activated form of RecA functions as a coprotease and promotes the self-cleavage of LexA. Consequently,

LexA repressor levels decrease in the cell, leading to the induction of the SOS response regulon. The gene products of the SOS regulon are involved in a range of cellular functions critical for survival, adaptation, and DNA repair (2). Specifically, SOS induction triggers the expression of genes involved in nucleotide excision and recombination repair (*uvrABD*, *recN*, and *ruvCAB*), the removal of alkylation damage (*ada*, *alkAB*, and *aidB*), and translesion synthesis (*polB*, *dinP*, *umuDC*, and *dnaE2*) (3). In addition, the LexA regulon often activates species-specific cell cycle checkpoints that stall cellular development to allow sufficient time for DNA repair to occur (4). LexA also negatively autoregulates its own transcription and *recA* expression (5), thereby ensuring that the SOS response is rapidly turned off once genome integrity has been restored.

The two principal regulators of the SOS response, RecA and LexA, are evolutionarily well conserved and present in almost all free-living bacteria, including the ubiquitous Gram-positive *Actinomycetota* (previously *Actinobacteria*) (3). Prominent members of this phylum are the streptomycetes, which are renowned for their extraordinary potential to produce specialized metabolites of economic and medical importance (6). *Streptomyces* species are characterized by a sophisticated developmental life cycle that starts with the germination of spores. Emerging germ tubes grow by apical tip extension and hyphal branching to establish a dense vegetative mycelial network that scavenges for nutrients. In response to nutrient starvation, hyphae escape surface tension and grow upwards to form so-called aerial hyphae. These hyphae subsequently undergo reproductive cell division, resulting in the production of chains of equal-size unigenomic spores that are eventually released into the environment (7).

Streptomyces are commonly found in sediments, a heterogeneous and competitive habitat where they are constantly exposed to a range of environmental stressors, including genotoxic agents. Earlier studies showed that a *Streptomyces recA* null mutant is more sensitive to DNA-damaging agents and that DNA-damaging antibiotics can inhibit sporulation, suggesting the existence of an SOS-like stress response (8, 9). However, the underlying regulatory network that underpins such a stress response is not understood. Furthermore, work over the last 2 decades has revealed that the SOS motif recognized by LexA and the number of genes directly controlled by LexA vary between bacterial genera and cannot simply be predicted bioinformatically (2, 3).

In this work, we confirm the existence of the SOS response in *Streptomyces venezuelae*, one of the key model organisms for this genus (7, 10), and demonstrate that RecA and LexA are important for survival under DNA-damaging growth conditions. By combining global transcriptomic profiling and chromatin immunoprecipitation sequencing (ChIP-seq) analysis, we identified the LexA regulon and the core set of SOS genes involved in DNA repair. Using surface plasmon resonance (SPR), we determined the LexA binding kinetics to selected target promoters and confirmed the specific interaction of LexA with the identified SOS box. Our *in vivo* and *in vitro* work further reveals that in *S. venezuelae*, LexA displays a differential DNA binding affinity that implies a fine-tuned activation of the SOS regulon in response to DNA damage.

RESULTS

Deletion of *recA* and *lexA* affects sporulation and sensitizes *S. venezuelae* to DNA damage. The *S. venezuelae* genome contains a single *recA* gene (*vnz_26845*) and a single *lexA* gene (*vnz_27115*). To characterize the SOS response in *S. venezuelae*, we first constructed a Δ*recA* mutant by replacing the *recA* coding region with an apramycin resistance cassette. Deletion of *recA* resulted in a growth defect and the formation of two colony types: minute nonviable colonies and slow-growing colonies with delayed and irregular sporulation septation. A similar Δ*recA* phenotype was previously described for *Streptomyces coelicolor* (8). The developmental defects of the Δ*recA* mutant could be fully complemented by expressing *recA* in *trans* from its native promoter (Fig. 1A; see Fig. S1A in the supplemental material). To exclude the possibility that a compensating mutation allowed for more robust growth in the slow-growing Δ*recA* mutant, we sequenced the genomic DNA isolated from two representative colonies and the parental strain. We did not detect a suppressor mutation in the Δ*recA* mutant,
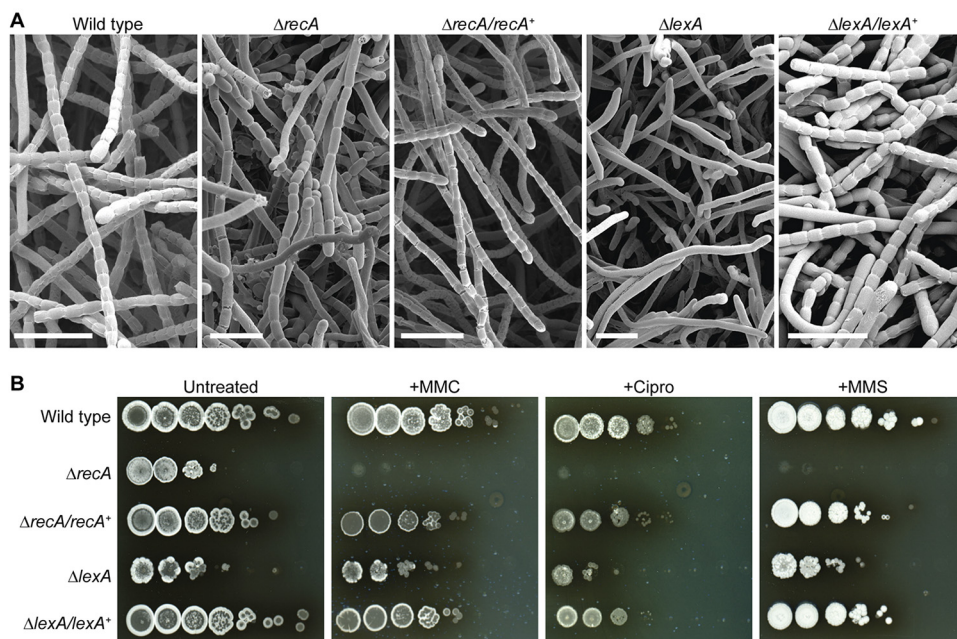
FIG 1 Deletion of *recA* and *lexA* impairs cellular development and increases sensitivity to DNA-damaging agents in *S. venezuelae*. (A) Representative cryo-scanning electron micrographs showing aerial hyphae from the wild type, the Δ*recA* mutant (KS3), the Δ*lexA* mutant (KS44), and the Δ*recA/recA*⁺ (KS14) and Δ*lexA/lexA*⁺ (KS57) complemented mutant strains. Scale bars, 5 μm. (B) Viability of the same strains described above when grown on solid MYM in the absence and presence of 0.25 μg mL⁻¹ mitomycin C (MMC), 3 μg mL⁻¹ ciprofloxacin (Cipro), and 3 mM methyl methanesulfonate (MMS). Equal concentrations of spores were used, and a 10-fold serial dilution series of the spore suspension was spotted onto MYM agar and incubated for 3 to 4 days. Shown are representative images from biological triplicate experiments.

suggesting that both colony phenotypes are a direct consequence of the *recA* deletion.

Next, we generated an *S. venezuelae lexA* null mutant. Using a three-step procedure, a second copy of *lexA* was first integrated at the phage BT1 attachment site of wild-type *S. venezuelae*, followed by the deletion of the native *lexA* gene and the insertion of an apramycin resistance cassette. The apramycin-marked Δ*lexA* allele was then moved back into wild-type (WT) *S. venezuelae*, which lacked a second copy of *lexA*, using generalized SV1 phage transduction, generating the Δ*lexA* mutant strain. Notably, deletion of *lexA* resulted in a severe growth defect and a "white" phenotype (Fig. S1A), indicating that sporulation was impaired in this genetic background. Scanning electron micrographs of colony surfaces confirmed that the Δ*lexA* mutant failed to deposit regularly spaced sporulation septa, resulting in undifferentiated aerial hyphae and virtually no spores (Fig. 1A). Normal sporulation and pigmentation were restored to the Δ*lexA* mutant when a single copy of wild-type *lexA* under the control of its native promoter was introduced in *trans* (Fig. 1A; Fig. S1A).

We then determined the viability of the wild type, the Δ*recA* mutant, the Δ*lexA* mutant and the corresponding complemented mutant strains in the presence of DNA-damaging agents, including mitomycin C (MMC), ciprofloxacin (Cipro), and methyl methanesulfonate (MMS). MMC and MMS are DNA-alkylating agents that cause DNA double-strand breaks, while ciprofloxacin targets DNA gyrase and inhibits DNA replication, leading to the accumulation of single-stranded DNA. For this, we either performed multiwell-based liquid growth assays or spotted serial dilutions of the individual strains onto solid medium supplemented with MMC, ciprofloxacin, or MMS. Based on our initial liquid growth assays, we found that treatment of wild-type *S. venezuelae* with 0.25 μg mL⁻¹ MMC, 3 μg mL⁻¹ ciprofloxacin, and 3 to 5 mM MMS strongly inhibited growth (Fig. 1B; Fig. S1B). As expected, the absence of either *recA* or *lexA* dramatically reduced the viability of *S. venezuelae* when grown in the presence of MMC, ciprofloxacin, or MMS, and thus, as in other bacteria, RecA and LexA are essential for the survival of genotoxic stress in *S. venezuelae*.
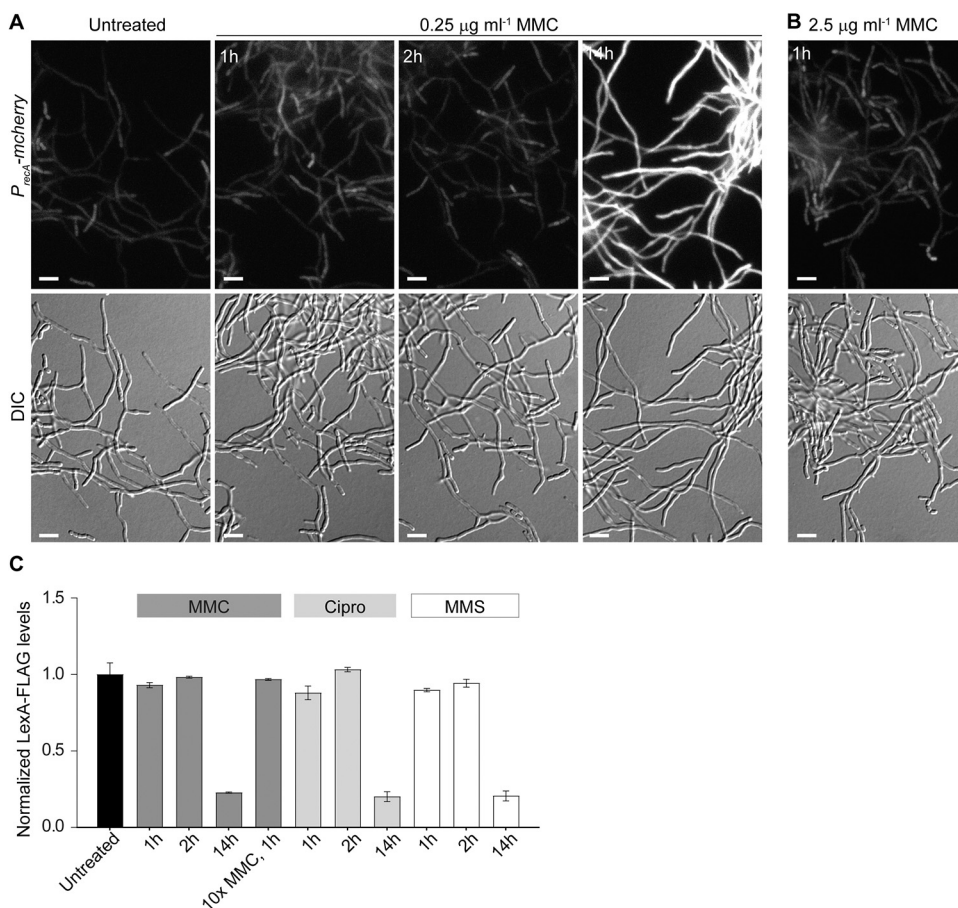
FIG 2 Induction of the SOS response requires prolonged exposure to DNA-damaging agents. (A and B) Fluorescence micrographs and corresponding differential interference contrast (DIC) images showing the induction of the *recA-mcherry* promoter fusion (P*_{recA}*-mcherry) in wild-type *S. venezuelae* hyphae (KS80) grown in the absence and presence of (A) 0.25 μg mL^{-1} mitomycin C (MMC) for 1, 2, and 14 h or (B) with 2.5 μg mL^{-1} mitomycin C for 1 h. Shown are representative images from biological triplicate experiments. Scale bars, 5 μm. (C) Automated Western blot analysis of LexA-FLAG protein levels in *S. venezuelae* (Δ*lexA*/*lexA*-FLAG$^+$ [KS74]) grown without and with 0.25 μg mL^{-1} and 2.5 μg mL^{-1} MMC, 3 μg mL^{-1} ciprofloxacin (Cipro), and 5 mM methyl methanesulfonate (MMS) for 1 h, 2 h, and 14 h. LexA-FLAG abundance was determined using a monoclonal anti-FLAG antibody. Protein levels were normalized to the untreated control samples. Analysis was performed in biological duplicate. Representative virtual Western blots are shown in Fig. S4A.

Induction of the SOS response requires prolonged exposure to DNA-damaging agents. The *Streptomyces* life cycle includes a multicellular growth phase, during which growing multinucleoid filaments are segmented by cross-walls. To gain an initial insight into the spatial and temporal activation of the SOS response within the mycelium, we constructed a strain in which expression of an ectopically inserted copy of *mcherry* was driven by the *recA* promoter and monitored the increase of mCherry fluorescence in response to MMC-induced DNA damage. We found that exposure of vegetative growing *S. venezuelae* cells to 0.25 μg mL^{-1} MMC for 1 h or 2 h did not lead to marked activation of the P*_{recA}*-mcherry reporter fusion. However, when *S. venezuelae* was grown in the presence of MMC for 14 h, a clear increase in cytoplasmic mCherry fluorescence within the entire mycelium was detectable (Fig. 2A). Notably, we obtained similar results when treating *S. venezuelae* with 3 μg mL^{-1} ciprofloxacin or 3 mM methyl methanesulfonate for 1 h or 14 h, respectively, indicating that the delayed induction of *recA* expression was not specific to mitomycin C (Fig. S2A). We also repeated the live-cell imaging experiments using a 10-fold-higher MMC concentration (2.5 μg mL^{-1}) to test if this would trigger a more rapid induction of the SOS response, but we did not detect increased expression of the *recA-mcherry* promoter fusion (Fig. 2B).
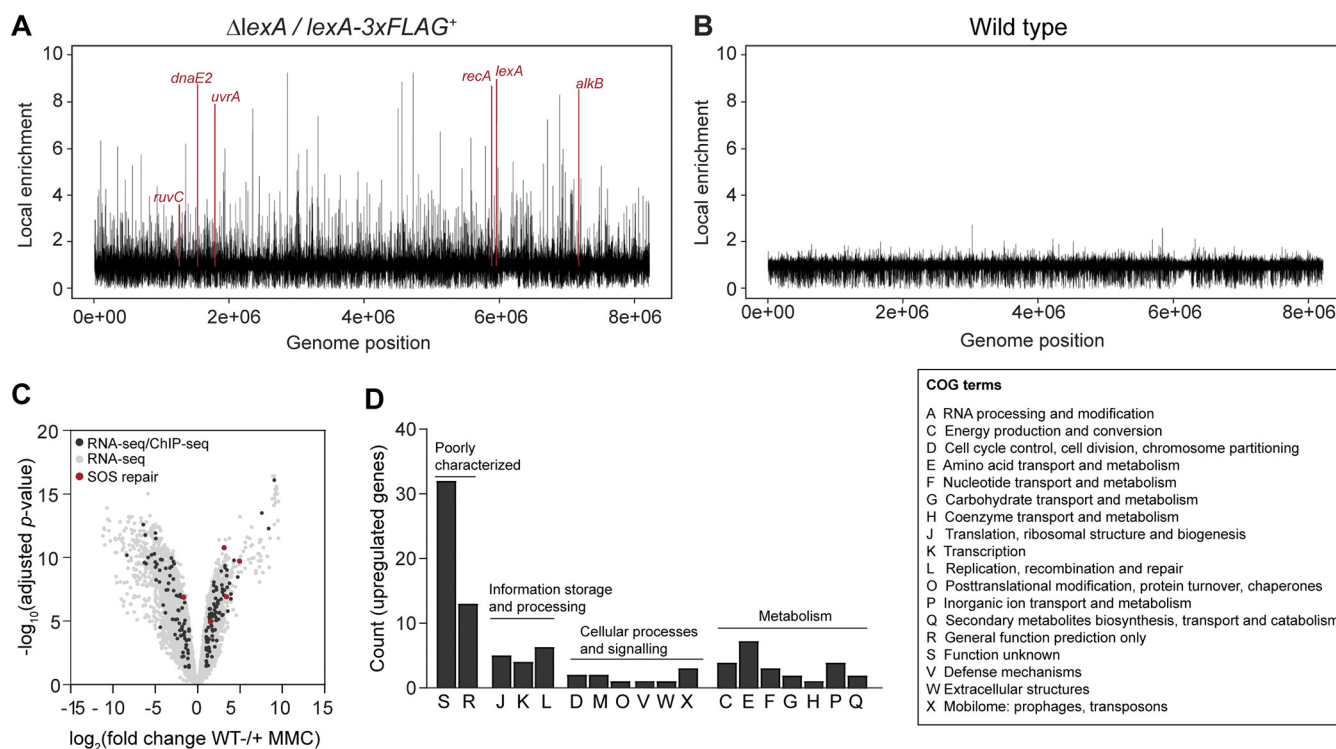
FIG 3 Genome-wide identification of the LexA regulon. (A and B) Genome-wide ChIP peak distribution of the LexA regulon in the (A) Δ*lexA*/*lexA*-FLAG⁺ strain (KS74) and (B) wild type. Strains were grown for 14 h in MYM. Peaks of selected LexA regulon genes involved in DNA repair are labeled and colored in red. ChIP-seq results were obtained from biological replicate experiments. (C) Volcano plot comparing RNA-seq profiles of the wild type grown with or without 0.25 μg mL^{-1} MMC for 14 h. Differentially expressed genes (gray dots) are defined by the adjusted P value ($P < 0.05$) and a fold change cutoff (|log$_2$ fold change| > 1). LexA target genes identified by ChIP-seq are labeled in black ($n = 175$). Red dots indicate core DNA repair genes in the SOS regulon (Table 1). RNA-seq data were obtained from biological triplicate experiments. (D) Functional classification of genes that were upregulated following the degradation of LexA in response to MMC-induced stress ($n = 97$; log$_2$ fold change > 1; adjusted $P < 0.05$) were assigned COG (Cluster of Orthologous Groups) identifiers, and their distribution was plotted. A legend for the corresponding COG annotations is presented to the right of the graph. Source data used to generate panels A to D can be found in Tables S1, S3, and S4.

To corroborate these findings, we engineered a functional LexA-FLAG fusion that complemented the growth and sporulation defect in hyphae lacking *lexA* (Fig. S2B). Vegetatively growing cultures expressing a single copy of *lexA* fused to the 3×FLAG tag were challenged with 0.25 μg mL^{-1} MMC for 1 h, 2 h, or 14 h, and subsequently, LexA-FLAG abundance in the corresponding cell lysates was analyzed by automated Western blotting. In line with fluorescent *recA* reporter fusion results (Fig. 2A), the LexA-FLAG protein level remained largely stable following treatment with MMC, Cipro or MMS for 1 and 2h, respectively. However, LexA-FLAG was almost completely absent in cell lysates of samples grown in the presence of these genotoxins for 14 h (Fig. 2C). To test the possibility that the FLAG tag was responsible for the slow degradation of LexA-FLAG fusion, we used a polyclonal LexA antibody to examine the decrease in native LexA levels in wild-type *S. venezuelae* following the same MMC treatment. We observed the same slow decrease in native LexA levels as we saw in the strain producing the LexA-FLAG fusion, showing that the FLAG tag did not affect the rate of degradation of LexA (Fig. S2C). Together, these results indicate that the activation of the two key components involved in launching the SOS response requires a chronic exposure to genotoxic stress in *Streptomyces*.

Defining the LexA DNA damage response regulon. To identify genes directly under the control of LexA, we performed chromatin immunoprecipitation sequencing (ChIP-seq) using anti-FLAG antibody on the Δ*lexA* strain that expressed a functional LexA-FLAG fusion (Fig. S2C). Wild-type *S. venezuelae* was used as a negative control to eliminate any false signals that might arise from cross-reaction of the anti-FLAG antibody with other DNA binding proteins. ChIP-seq revealed numerous LexA binding sites distributed across the *S. venezuelae* genome in the absence of MMC (Fig. 3A). No significant

enrichment was observed in the wild-type control, suggesting that there was no cross-reaction of the anti-FLAG antibody leading to nonspecific enrichment (Fig. 3B). In total, 498 ChIP-seq peaks were identified, corresponding to LexA binding sites that were enriched more than 2-fold relative to the wild-type control. Of these, we selected all the binding sites that were located within a potential regulatory region of −200 to 100 bp relative to the start codon of the first gene in a transcriptional unit (Table S1). Through this route, we determined 270 putative LexA binding sites.

Furthermore, we detected 176 intragenic LexA binding sites that were in proximity to previously mapped transcription start sites (11), indicating that LexA might also control the activity of intragenic promoters. We note that the transcription start site mapping was performed in the absence of DNA damage, a condition during which LexA remains bound to its target operators and largely prevents transcription of the associated genes. Closer inspection of the putative intragenic promoters associated with LexA enrichment sites revealed that 6 out of the 176 putative intragenic promoters were located within genes with a proposed function in DNA replication and repair (*vnz_05400*, *vnz_06010*, *vnz_08430*, *vnz_25520*, and *vnz_29285*), and within one gene that shares similarity with the cell division protein ZapE (*vnz_29020*) (12). In addition, two noticeable intragenic LexA binding sites for which no transcription start site data are available were detected within the DNA helicase gene *uvrD* (*vnz_23895*) and the error-prone DNA polymerase gene *dnaE2* (*vnz_06640*) (Table S2). However, with the exception of *dnaE2*, none of the genes associated with an intragenic LexA binding site were differentially regulated in response to DNA damage (Table S3).

In order to identify LexA target genes that showed a clear transcriptional response to DNA damage, we performed transcriptome sequencing (RNA-seq) on wild-type *S. venezuelae* treated with 0.25 μg mL^{-1} MMC combined with an untreated wild-type control. Because we observed significant induction of *recA* expression and LexA degradation only after prolonged exposure to MMC, we conducted RNA-seq in three independent biological samples obtained from cultures that were grown in the presence and absence of MMC for 14 h. Due to the severely reduced viability of the Δ*recA* mutant when grown in medium containing MMC (Fig. 1B), we were unable to include this strain in the RNA-seq analysis. In this way, we identified 175 LexA binding sites that were associated with differentially expressed transcriptional units upon treatment with MMC (adjusted $P < 0.05$, |log$_2$ fold change| > 1) (Fig. 3C; Table S3). Of these, 97 transcriptional units were upregulated, including one putative LexA target of unknown function located on the *S. venezuelae* plasmid pSVJI1, and 78 transcriptional units were downregulated following MMC treatment (10). Although LexA generally functions as transcriptional repressor (13–15), the MMC-induced downregulation of genes associated with a LexA binding site is indicative of a direct or indirect positive regulation of these genes by LexA. We note that our global transcriptional profiling analysis further showed that several genes required for sporulation were significantly downregulated following the treatment with MMC, including the classical *Streptomyces* developmental regulatory genes *whiI*, *whiH*, and *whiB*, genes involved in cell division (*ssgB*) and chromosome segregation (*smeA-sffA*) and several genes within the *whiE* locus, which encodes the biosynthesis machinery for the production of the polyketide pigment associated with mature spores (16–19). These findings are in agreement with those of other recent studies, reporting that subinhibitory concentrations of MMC inhibit sporulation in *S. venezuelae* (9, 20).

Functional categorization of the 97 LexA target genes derepressed in response to MMC stress did not suggest an enrichment of a specific gene category and revealed that the functions of most genes associated with a LexA binding site are unknown (Fig. 3D and Table 1). Among the LexA targets that showed the highest upregulation were several genes belonging to a predicted prophage cluster (*vnz_21525*, *vnz_21545*, and *vnz_21550*) and genes functioning in protein translation and degradation (*vnz_05845* and *vnz_00275*), metabolism (*vnz_22770*), and molecule transport (*vnz_15995* and *vnz_26265*). Importantly, our integrated RNA-seq and ChIP-seq approach led to the identification of a core set of

TABLE 1 Selected members of the SOS regulon and coregulated genes

| Gene | Locus | Description | FC[a] | | SOS box | Position (bp)[b] |
			RNA-seq	ChIP-seq		
Information storage and processing						
recA	vnz_26845	Recombinase A and LexA coprotease	9.07	1.84	TCGAACATCCATTC[c]	−162
recX	vnz_26850	Recombination regulator	6.28			
lexA	vnz_27115	Transcriptional repressor	−3.10	1.34	TCGAAAGGTTGCGC (lexA-1)[c]	−53
					TCGAACGTGTGTTT (lexA-2)[c]	
dnaE2	vnz_06640	DNA polymerase III, α subunit	30.62	1.39	TCGTACGTACGTTC (dnaE2-1)[c]	−68
dinP	vnz_06635	DNA polymerase IV	13.74		TCGAACGTCCGTAC (dnaE2-2)[c]	
ruvC	vnz_05440	Resolvase endonuclease subunit	2.78	1.84	TCCACCCCGAGAAC[c]	−23
ruvA	vnz_05435	Holliday junction DNA helicase	2.13	1.84		
alkB	vnz_32390	Alkylated DNA repair protein	11.02	1.39	GGTTACGCTGGATC[c]	−20
infC	vnz_05845	Translation initiation factor IF-3	3.05	2.39	TCGTACTCCTGTGC	91
parE	vnz_27225	DNA topoisomerase IV subunit B	3.78	1.18	TCGAACTTACGTCC	−157
Cellular processes and signaling						
	vnz_21525	Phage tail fiber protein	526.40	2.24	TCGAACACCGGCGC	−174
	vnz_21545	Hypothetical protein	190.02	1.00	TCGAACACAAGGCC	−123
	vnz_21550	Hypothetical protein	190.02	1.00	TCGAACACAAGGCC	−182
	vnz_00275	Serine protease	10.93	1.92	TCGAACGTTTGACG	−42
Metabolism						
	vnz_22770	Alcohol dehydrogenase	26.72	1.62	CCGGACACCGGGAC	−105
	vnz_15995	ABC transporter permease	15.14	2.01	CCGAACGCATGTGT	−30
	vnz_26265	Thiamine ABC transporter substrate-binding protein	9.00	1.79	TCGAACACATCTCC	−199
General prediction						
	pvnz_37140	Hypothetical protein	15.35	1.22	TCGAACACGTGCTC	−14
	pvnz_37135	DNA polymerase IV	7.52			
	vnz_31145	Radical SAM protein	19.97	1.31	TCGACCGTTCGCTC	−61

[a]For RNA-seq data, relative fold changes (FC) represent gene expression of the wild-type cells grown for 14 h in the presence of MMC (WT plus MMC) compared to untreated cells (WT minus MMC) (adjusted $P < 0.05$). For the Chip-seq data, relative FC represent local LexA-FLAG enrichment of cells expressing *lexA*-FLAG, which were grown for 14 h in the absence of MMC (LexA-FLAG minus MMC) compared to cells grown in the presence of MMC (LexA-FLAG plus MMC) ($|\log_2$-FC$| > 1$).
[b]The position of the first base of the SOS box relative to the predicted start codon is indicated.
[c]SOX box experimentally validated (Fig. 4D).

LexA targets (3), including the *recA-recX* operon, *lexA*, and several conserved DNA repair genes encoding the translesion DNA polymerases DnaE2 and DinP, RuvC and RuvA required for recombination and repair, and the alkylation repair protein AlkB. In addition, our data suggest that *uvrA* (nucleotide excision repair) may also be part of the LexA-controlled DNA damage response as we observed a clear LexA ChIP-seq peak and a change in *uvrA* expression, although this was just beneath our applied cutoff in the RNA-seq analysis ($|\log_2$ fold change$| > 1$).

Moreover, the LexA regulon includes additional genes that could further contribute to the relief of DNA damage stress. These genes include *parE* (*vnz_27225*), which encodes an additional topoisomerase IV subunit, *vnz_31145*, which shares similarity to radical *S*-adenosylmethionine (SAM) enzymes that repair DNA cross-links between thymine bases caused by UV, radiation and an operon located on *S. venezuelae* plasmid pSVJI1 consisting of a hypothetical protein and an error-prone DNA polymerase gene (*pvnz_37140* to *pvnz_37135*).
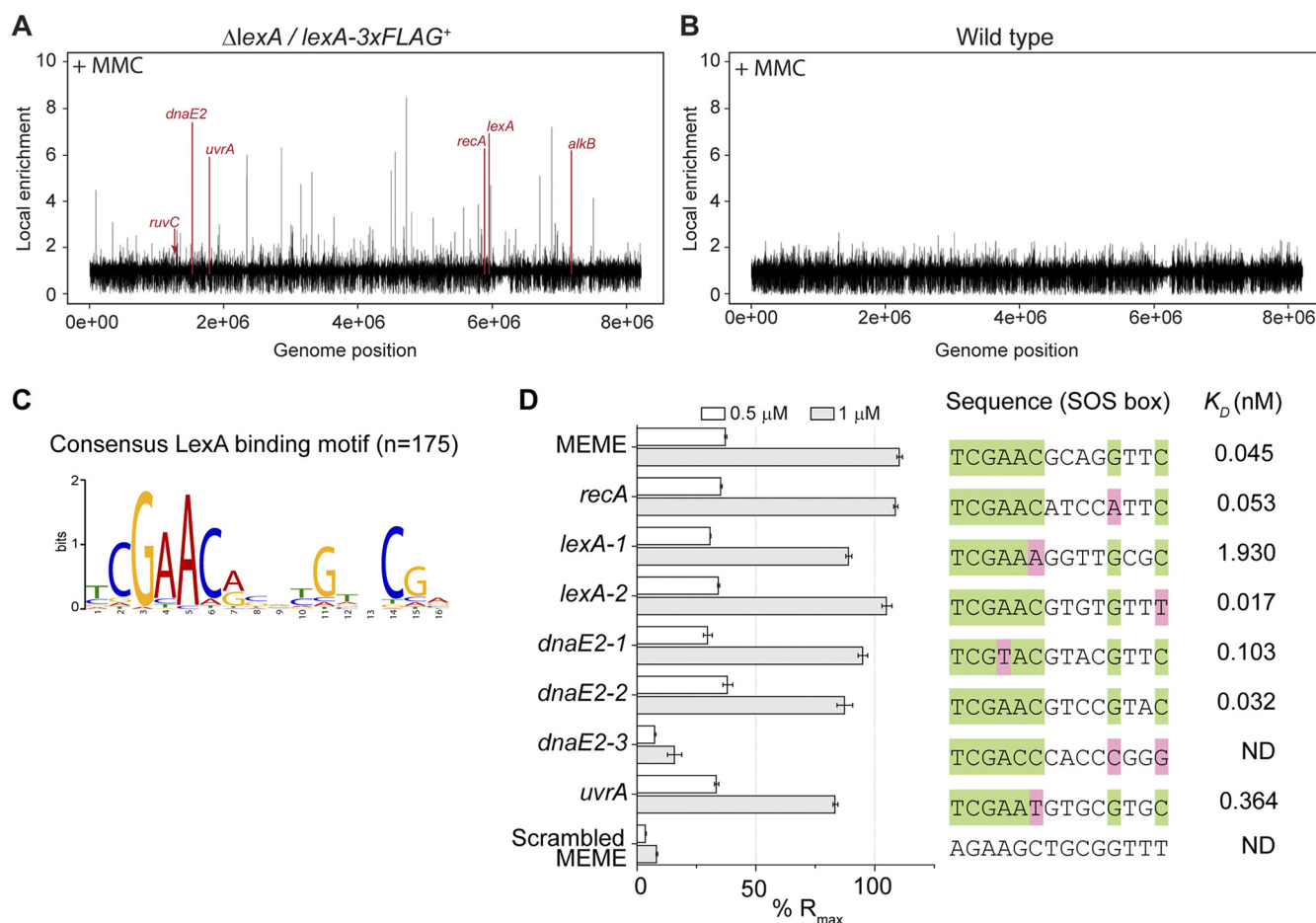
FIG 4 LexA binds tightly to SOS boxes of core DNA damage genes *in vitro*. Genome-wide ChIP peak distribution of the LexA regulon in the (A) Δ*lexA*/*lexA*-FLAG⁺ strain (KS74) and (B) wild type. Strains were grown for 14 h with 0.25 μg mL^{-1} MMC. Peaks of selected LexA regulon genes are labeled and colored in red. (C) Identification of the LexA consensus motif (E value of 1.0e−252) by the MEME algorithm. The input of the analysis comprised ChIP-seq sequences with a length of 100 nt. The total number of sequences (*n*) is indicated. (D) Surface plasmon resonance (SPR) was used to determine the binding kinetics of LexA (0.5 μM and 1 μM) to 23-bp double-stranded DNA that contained individual target sequences located upstream of SOS genes involved in DNA repair. The target sequences (SOS box) used in these experiments are presented. Highly conserved nucleotides are shown in green, and mismatches to the LexA consensus motif are shaded in magenta. A wider range of LexA concentrations was used to determine the binding affinity (K_D) of LexA to the individual target sequences (Fig. S3). The affinities for the *dnaE2-3* binding site and the scrambled MEME motif were not determined (ND) due to very little specific binding of LexA.

SOS boxes of DNA damage repair genes are tightly bound by LexA.

Since the SOS response involves the derepression of LexA target genes, we sought to study the effect of MMC treatment on LexA binding *in vivo*. Therefore, and in parallel with our earlier experiments conducted under non-DNA-damaging growth conditions, we performed ChIP-seq experiments following MMC-induced stress and subsequently compared LexA enrichment across the genome in untreated samples to that in ChIP-seq samples that had been obtained from cultures grown in the presence of 0.25 μg mL^{-1} MMC for 14 h. In contrast to our untreated ChIP-seq experiments, which demonstrated widespread binding of LexA across the genome, there was an observable decrease in genome-wide LexA binding in the presence of MMC (Fig. 4A). This is in line with the observation that LexA protein levels are decreased under DNA-damaging conditions (Fig. 2C). As in our earlier experiments, no significant enrichment was observed in the wild-type negative control under these conditions (Fig. 4B). Of the 175 LexA binding sites determined here to be part of the SOS response, MMC treatment resulted in reduced local enrichment of LexA at 112 genomic positions and the complete dissociation of LexA at 61 chromosomal loci. Both sets of loci also included the core DNA damage repair genes described above (Table 1; and Fig. S3A). Two chromosomal loci retained a similar level LexA enrichment under the conditions tested (Table S4).

These findings prompted us to further examine the sequence specificity of LexA binding. Using the motif-based sequence analysis tool MEME (21) and 100-nucleotide (nt) sequences located under the summit of each LexA ChIP-seq peak ($n = 175$), we first identified the 16-bp consensus LexA DNA-binding motif tCGAAC-N_4-GNNCGa (Fig. 4C), which is an imperfect palindromic sequence, similar to previously reported LexA binding motifs from related and distant bacterial systems (3). We then compared this consensus LexA binding motif to the motifs generated from 100-nt sequences associated with either ChIP-seq peaks that decreased ($n = 112$) or disappeared ($n = 61$) after MMC stress. This analysis did not reveal any significant differences in the sequence specificity of LexA binding *in vivo* (Fig. S3B), indicating that additional factors might contribute to LexA enrichment and the differential response to MMC.

To further validate our *in vivo* ChIP-seq analysis, we examined the DNA binding specificity of purified *S. venezuelae* LexA using surface plasmon resonance (SPR). Twenty-three-base-pair double-stranded oligonucleotides containing the consensus LexA DNA binding motif were tethered to a chip surface within an SPR flow cell. Purified His_6-LexA was flowed over the test DNA, and LexA binding was recorded by measuring the change in response units during LexA injection. Control experiments using double-stranded DNA with a scrambled LexA DNA binding sequence showed only a very weak association of LexA, supporting the idea that the observed binding was sequence specific (Fig. 4D). In addition, we performed SPR analysis using 23-bp duplex DNA that contained the putative LexA binding motifs identified upstream of *lexA*, *recA*, and the two SOS genes *dnaE2* and *uvrA*. Based on our initial MEME analysis, we identified two potential LexA binding sites in the promoter region of *lexA* (*lexA1* and *lexA2*) and three for *dnaE2* (*dnaE2-1*, *dnaE2-2*, and *dnaE2-3*). In agreement with our ChIP-seq results, we observed clear binding of LexA to the predicted binding sites, except for the *dnaE2-3* motif, suggesting that either this sequence may not represent a relevant LexA binding site or an additional factor or factors are required for binding *in vivo* (Fig. 4D). We repeated the SPR experiments, using sequentially increasing concentrations of LexA to enable the determination of the binding affinity equilibrium dissociation constant (K_D). These analyses showed a differential but overall strong binding of LexA to the tested duplex DNA, indicating that the induction of LexA target genes *in vivo* is under tight control in *Streptomyces* (Fig. 4D; Fig. S3C). This may provide an explanation for the requirement of prolonged exposure to genotoxic agents to induce the SOS response in *S. venezuelae* since LexA needs to first disassociate from its target sequence to become susceptible to RecA-stimulated self-cleavage (22). However, we cannot exclude the possibility that the overall stability of LexA also contributes to the delayed induction of the SOS response.

DISCUSSION

In this work, we confirm the presence of a functional DNA damage response and identify the core set of LexA-controlled SOS genes in *S. venezuelae*. While deletion of *recA* is not detrimental for most bacteria under non-DNA-damaging growth conditions, deletion of *lexA* and the resulting constitutive activation of the SOS response are lethal in *Escherichia coli* or cause cell filamentation in other bacterial species (23–26). *S. venezuelae* strains lacking either *recA* or *lexA* are viable; however, growth and sporulation are severely compromised in these mutant strains even under non-DNA-damaging conditions. Available microarray data indicate that *recA* is constitutively expressed throughout the *S. venezuelae* life cycle (27). Given the importance of *recA* in genome maintenance (28), it is likely that the observed phenotypic defects in the *recA* mutant are a direct consequence of genome instability, which could result in a large deletion in the chromosomal arms or defective chromosome segregation (8, 29). Furthermore, in the *lexA* null mutant, permanent induction of the SOS response may result in the activation of a cell cycle checkpoint that suppresses sporulation, analogous to the SOS-dependent cell division inhibitors identified in diverse bacteria (30–33). Notably, *Streptomyces* lack clear homologs of these known cell division regulators, indicating

the presence of a yet unidentified mechanism involved in coordinating DNA damage repair and cell division.

Our investigations revealed that the activation of the SOS response is delayed and requires a chronic exposure to DNA-damaging agents in *S. venezuelae*. Similar slow activation of the SOS response was previously reported for other *Streptomyces* species and related *Actinomycetota*, showing that short treatments with DNA-damaging agents were not sufficient to increase *recA* expression (34–36). The basis for this phenomenon is not fully understood, but several factors may contribute to the delayed induction of the SOS response. For example, the basal level of RecA may be sufficiently high to repair DNA damage caused by short-term genotoxic stress without the need to induce the SOS response. It is also conceivable that LexA autocleavage is intrinsically slow compared to LexA from other organisms in which LexA is degraded within minutes (37, 38). It is also conceivable that the coprotease function of RecA is inhibited by RecX, a negative regulator of RecA activity (36, 39). Although we cannot exclude the possibility that the intracellular accumulation of genotoxic agents is slowed down by increased efflux activity or properties of the *Streptomyces* cell envelope that limit the uptake of toxic compounds, these findings suggest that the regulation of the SOS response might be different in *Streptomyces*. Notably, the related *Actinomycetota* species *Mycobacterium smegmatis* employs two DNA damage response pathways, a RecA/LexA-dependent SOS response and a RecA/LexA-independent DNA damage response, with the latter one controlling the vast majority of DNA repair genes (40, 41). This alternative stress response involves a protein complex comprised of the two transcriptional regulators PafB and PafC, which bind to a DNA sequence motif that is distinct from the SOS box to activate the mycobacterial DNA damage response, presumably upon binding single-stranded DNA (40–42). Although *Streptomyces* species encode homologs of the PafBC system, an initial motif search suggested that the PafBC binding motif from *M. smegmatis* is not conserved in *S. venezuelae*. Thus, it remains to be shown whether a similar RecA/LexA-independent DNA response exists in *Streptomyces*.

Our results, however, establish the presence of a LexA-dependent DNA damage response in *Streptomyces*. In total, we identified 175 LexA binding sites that were associated with DNA damage-responsive genes that were either upregulated or downregulated following MMC-induced degradation of LexA. While the majority of these genes are of unknown function, about 36% of all differentially regulated genes are predicted to encode proteins involved in metabolism, signaling, and other cellular processes. This clearly highlights the functional diversity of the gene categories that comprise the LexA regulon in *Streptomyces*. Importantly, our work identifies a core set of SOS-regulated DNA response genes involved in the regulation of the SOS response (*lexA* and *recA)*, DNA mutagenesis (*dnaE2-dinP*), and DNA repair (*ruvC-ruvA* operon and *alkB*) (3). We also identified several additional genes and previously unrecognized LexA target genes, involved in DNA decatenation (*parE*) (43, 44), UV damage repair (*vnz_31145*) (45), and mutagenesis (*pvnz_37140* to *pvnz_37135*), which could further contribute to restoring the integrity of the genome.

Furthermore, we detected a significant number of positively regulated LexA targets. Although we cannot exclude the possibility that the MMC-induced downregulation of LexA target genes might reflect the requirement for an additional transcriptional regulator or regulators for induction, several examples of positive regulation by LexA have now been identified, (23, 46–49). Two noticeable LexA targets in *S. venezuelae* that showed a significant downregulation upon MMC treatment include the structural genes for the developmental regulator WhiI and the small membrane protein SmeA, which together with its partner protein SffA, is involved in chromosome segregation during sporulation (18, 50). However, *whiI* and *smeA* expression is also controlled by additional developmental regulators, indicating the presence of a multilayer regulatory network that controls the initiation of sporulation (16, 51). Together, our findings support the idea of a much more diverse cellular role of LexA in DNA damage stress resistance and *Streptomyces* development.

Our work further revealed that LexA displays a differential binding behavior *in vivo*, indicating a graded response to DNA damage. These observations are in line with a

hierarchical induction of LexA targets that is dependent upon both the level of DNA damage and the LexA dissociation rate constant at a given promoter (52–54). Indeed, our *in vitro* assays confirmed that in *S. venezuelae*, LexA binds tighter to the *recA*, *lexA2*, and *dnaE2-2* operator sequences than the *lexA1/dnaE2-1* motif and the SOS box located in the promoter region of *uvrA*. This is likely to create a finely tuned response, balancing DNA damage surveillance, rapid repair of DNA lesions, and the need to mount a full SOS response. Collectively, our work provides significant insight into the SOS response and how it might enable *Streptomyces* to survive in diverse environments.

MATERIALS AND METHODS

Bacterial strains and growth conditions. The strains, plasmids, and oligonucleotides used in this work are listed in Tables S5 and S6 in the supplemental material. *E. coli* strains were grown in LB or LB agar at 37°C supplemented with the following antibiotics when necessary: 100 μg mL^{-1} carbenicillin, 50 μg mL^{-1} kanamycin, 25 μg mL^{-1} hygromycin, 50 μg mL^{-1} apramycin, or 25 μg mL^{-1} chloramphenicol. *S. venezuelae* NRRL B-6544 was grown in maltose-yeast extract-malt extract medium (MYM), composed of 50% tap water and 50% reverse-osmosis water, and supplemented with R2 trace element (TE) solution at a ratio of 1:500. Liquid cultures were grown under aeration at 30°C and at 250 rpm. MYM agar was supplemented with the following antibiotics when required: 5 μg mL^{-1} kanamycin, 25 μg mL^{-1} hygromycin, or 50 μg mL^{-1} apramycin.

Construction and complementation of the *recA* null mutant. The Δ*recA* mutant strain (KS3) was generated using "redirect" PCR targeting (55, 56). The *recA* coding sequence (*vnz_26845*) on the cosmid vector PI1-B2 (http://strepdb.streptomyces.org.uk/) was replaced by an *oriT*-containing apramycin resistance cassette, which was amplified from pIJ773 using the primer pair ks6 and ks7. The resulting disrupted cosmid (pKS100) was introduced into *S. venezuelae* by conjugation via *E. coli* ET12567/pUZ8002. The resulting exconjugants were screened for double-crossover events (Apr^r Kan^s), and deletion of *recA* was verified by PCR analysis using the primers ks8, ks9, and ks10. A representative *recA* null mutant was designated KS3. For complementation, plasmid pKS2 (P_{recA}-*recA*) was introduced into the Δ*recA* mutant by conjugation.

Genomic DNA for genome sequencing of the Δ*recA* mutant (KS3) and the parental wild-type strain was performed using the FastDNA kit for soil (MP Biomedicals Germany). Genomic DNA of biological replicate samples per strain was sequenced by MiGS (Pittsburgh, USA).

Construction and complementation of the *lexA* null mutant. To generate the Δ*lexA* mutant strain (KS44), a plasmid carrying a second copy of *lexA* (pKS1) was first integrated at the phage BT1 attachment site of wild-type *S. venezuelae*. In the resulting strain (KS9), the native *lexA* coding sequence (*vnz_27115*) was then replaced by the *apr-oriT* cassette using the Redirect PCR targeting technology and cosmid PI2-B2 as described above, using the primer pair ks1 and ks2 to PCR amplify the *apr-oriT* cassette from pIJ773. The mutagenized cosmid (pKS200) was introduced into KS9 by conjugation via ET12567/pUZ8002, and exconjugants that had successfully undergone double-crossover events were identified by screening for apramycin resistance and kanamycin sensitivity, yielding strain KS25. The Δ*lexA::apr* allele of KS25 was then moved back into wild-type *S. venezuelae* via generalized SV1 phage transduction, as described by Tschowri et al. (57). Transduction of the Δ*lexA::apr* allele was confirmed by PCR analysis using the primers ks3, ks5, and ks32. A representative Δ*lexA* null mutant strain was designated KS44. For complementation, plasmid pKS1 (P_{lexA}-*lexA*) or pKS3 (P_{lexA}-*lexA*-3×FLAG) was introduced into the Δ*lexA* mutant by conjugation, yielding strains KS57 and KS74, respectively.

RNA preparation, sequencing (RNA-seq), and analysis. RNA-seq was conducted in biological triplicate using the protocol described by Bush et al. (58). Triplicate cultures of wild-type *S. venezuelae* were grown in 30-mL MYM cultures with shaking (250 rpm) for 14 h at 30°C; "treated" cultures were grown with the addition of 0.25 μg mL^{-1} mitomycin C (MMC) (Merck Life Sciences UK, Ltd.). Mycelial pellets from untreated and treated cultures were washed in 1× phosphate-buffered saline (PBS) before lysis and RNA purification using the RNEasy kit (Qiagen). Purified RNA samples were treated with on-column DNase I (Qiagen), followed by an additional DNase I treatment (Turbo DNA-free; Invitrogen), and the absence of DNA contamination was confirmed by PCR amplification of the housekeeping gene *hrdB* (*vnz_27210*) using the primer pair mb1 and mb2. Library construction, rRNA depletion and paired-end Illumina Hiseq sequencing (2× 150-bp configuration) was performed by Genewiz (NJ, USA).

The quality of the obtained sequencing reads was checked using FastQC (https://www.bioinformatics.babraham.ac.uk/projects/fastqc/) and the reads were mapped to the genome of *S. venezuelae* NRRL B-65442 (NCBI reference sequence NZ_CP018074.1) using the Bowtie2 alignment tool (59) and subsequently sorted and indexed using the Samtools package (60). A custom Perl script was used to make a saf file for genes in the *S. venezuelae* genome. The featureCounts tool of the BioConductor package "Rsubread" was used to count the reads mapping to every gene in the *S. venezuelae* genome. The counts were read into a DGEList object of the edgeR package of R, and a quasilikelihood negative binomial generalized log-linear model was fitted to the data using the glmQLFit function of edgeR. Genewise statistical tests were conducted using the glmQLFTest function of edgeR (61). The "topTags" function was used to arrive at a table of differentially expressed genes (61). Genes were classed as differentially expressed genes (DEGs) if the log$_2$ fold change (treated/untreated) was greater than or equal to 1 or less than or equal to −1 and had a false-discovery rate (FDR [adjusted *P* value]) of ≤0.05.

Chromatin immunoprecipitation sequencing and analysis. ChIP-seq was performed in biological replicates as described previously (16) using a *S. venezuelae* Δ*lexA* strain that was complemented with a *lexA*-3×FLAG fusion (KS74). Cells were grown in MYM in the absence (untreated) and presence of 0.25 μg mL^{-1} MMC for 14 h (14-MMC) at 30°C. Library construction and sequencing were performed by Genewiz (NJ, USA) using Illumina Hiseq (2× 150-bp configuration, trimmed to 100 bp). Obtained sequencing reads were aligned to the *S. venezuelae* NRRL B-65442 genome (NCBI reference sequence NZ_CP018074.1) using the Bowtie 2 alignment tool (59). The resultant bam files were sorted and indexed using the Samtools package (60). A custom Perl script was used to make a saf file for every 30-nucleotide section in the *S. venezuelae* genome, with adjacent sections overlapping by 15 nucleotides. The featureCounts tool of the R package Rsubread was used to count the number of reads mapping to every 30-nucleotide section in the saf file made above. A custom R script was then employed to calculate a local enrichment for every 30-nucleotide section (overlapping by 15 nucleotides) by comparing the read density in the section to the read density in the 3,000 nucleotides around the section. The local enrichment in the corresponding sections of the controls were subtracted from the local enrichment of the ChIP samples. Custom Perl and R scripts were used to list out genes to the left and right and overlapping genome sections with a local enrichment of 2 or more. In addition, genes had to be in the right orientation and within 300 nucleotides of the enriched region for association with LexA-3×FLAG binding sites. Intragenic LexA bindings sites (local enrichment of >2) were defined as genomic positions that were located more than 100 bp downstream of the annotated start codon of a gene and which were not considered to be part of a promoter region of the downstream gene. Of the 208 intragenic LexA-3×FLAG binding sites, 176 binding sites were detected in proximity of a transcription start site (based on the "14h" TSS data set publicly available at EMBL-EBI under E-MTAB-10690) (11).

To assess the effect of MMC, the enrichment of the 175 LexA-3×FLAG ChIP-seq peaks located upstream of transcriptional units was assessed based on the differential response to MMC stress (adjusted $P < 0.05$ and fold change cutoff |log$_2$ fold change| >1) and on the following criteria. (i) Complete dissociation of LexA-3×FLAG from a binding site upon MMC treatment was judged to have occurred when the enrichment value (log$_2$ fold change) in the MMC-treated ChIP-seq data set (LexA-3×FLAG 14-h MMC/WT 14-h MMC) was less than 0.25. (ii) No dissociation of LexA-3×FLAG from a binding site upon MMC treatment was called when the enrichment value (log$_2$ fold change) calculated from the comparison of the treated and untreated ChIP-seq data sets (LexA-3×FLAG 14-h MMC/LexA-3×FLAG untreated) was less than 0.2. (iii) Partial dissociation of LexA-3×FLAG from a binding site upon MMC treatment was defined when peaks displayed a local enrichment value (log$_2$ fold change) in the MMC-treated ChIP-seq data set (LexA-3×FLAG-14-h MMC/WT 14-h MMC) of more than 0.25 and the enrichment value (log$_2$ fold change) calculated from the comparison of the treated and untreated ChIP-seq data sets (LexA-3×FLAG 14-h MMC/LexA-3×FLAG untreated) was greater than 0.2.

Functional analysis of the LexA regulon. Analysis for the enrichment of functional classes was performed on proteins encoded by the 176 genes that were associated with intragenic LexA binding sites and the 175 differentially expressed genes that are subject to LexA regulation (Tables S2 and S4). To predict conserved protein features and to assign COG (Clusters of Orthologous Groups) identifiers, the queries were searched against the Position Specific Scoring Matrix (PSSM) database (NCBI) using the rpsblast program (62). Where more than one COG identifier was reported, genes were inspected for their genetic context and predicted function and were manually assigned a COG class.

Motif prediction from LexA enrichment sites. One-hundred-nucleotide sequences surrounding the center position of each of the 175 enrichment sites determined by our ChIP-seq analysis were used as input for the MEME suite (21) (Table S4), with an *S. venezuelae* background model, to search for a conserved LexA binding motif (SOS box). Site distribution was set to "zero" or "one occurrence per sequence," and the MEME algorithm was set to search for three motifs on both strands with a width of 6 to 500 nucleotides.

Automated Western blotting. To determine LexA and LexA-FLAG levels, the Δ*lexA*/*lexA*-3×FLAG strain (KS74), and the wild type were used. To confirm specific binding of the antibodies, the wild type and the Δ*lexA* deletion strain (KS44) were used as the respective negative controls. Duplicate cultures of each strain were grown in liquid MYM for 14 h without (untreated) and with 0.25 μg mL^{-1} MMC, 3 μg mL^{-1} ciprofloxacin, or 3 mM MMS. After 14 h, untreated cultures were exposed for 1 and 2 h to 0.25 μg mL^{-1} or 2.5 μg mL^{-1} MMC, 3 μg mL^{-1} ciprofloxacin, and 5 mM MMS, respectively. At the end of the incubation time, 2 to 5 mL of each MYM culture was removed and washed once with 1× PBS. Samples of mycelium were resuspended in 0.4 mL ice-cold sonication buffer (20 mM Tris [pH 8.0], 5 mM EDTA, 1× EDTA-free protease inhibitors [Sigma-Aldrich]) and sonicated (5 times for 15 s on and 15 s off) at an amplitude of 4.5 μm. Lysates were then centrifuged at 16,000 × *g* for 15 min at 4°C to remove cell debris. The total protein concentration was determined using the Bradford assay (Bio-Rad). To detect LexA-FLAG or LexA abundance in cell lysates, 2 μg of total protein for each sample was loaded in duplicate into a microplate (ProteinSimple 043-165) together with either anti-FLAG antibody (Sigma F4725) diluted 1:100 or polyclonal anti-LexA antibody diluted 1:200. LexA-FLAG and LexA levels were then assayed using the automated Western blotting (WES) machine (ProteinSimple, San Jose, CA), according to the manufacturer's guidelines. Virtual Western blots related to Fig. 2C and Fig. S2C were generated using the Compass software for simple Western (version 6.0.0), and uncropped images of representative blots are shown in Fig. S4.

Fluorescence microscopy. To visualize the expression of the P$_{recA}$-*mcherry* fusion in *S. venezuelae* (KS80), cells were grown in triplicate in liquid MYM with and without MMC, ciprofloxacin, and MMS as described. Cells obtained from each culture were immobilized on a 1% agarose pad and visualized using a Zeiss Axio Observer Z.1 inverted epifluorescence microscope fitted with an sCMOS camera (Hamamatsu Orca Flash 4), a Zeiss Colibri 7 LED light source, and a Hamamatsu Orca Flash 4.0v3 sCMOS camera. Images were acquired using a Zeiss Alpha Plan-Apo 100×/1.46 oil differential inference contrast (DIC) M27 objective

with an excitation/emission bandwidth of 577 to 603 nm/614 to 659 nm to detect fluorescence emitted by the mCherry reporter fusion. Still images were collected using the Zen Blue software and further analyzed using the Fiji imaging software (63). To normalize the mCherry fluorescence intensity across different MMC treatments, images were corrected for background fluorescence.

Cryo-scanning electron microscopy. *Streptomyces* samples were mounted on an aluminum stub using Tissue Tek (Agar Scientific, Ltd., Stansted, England) and plunged into liquid nitrogen slush. The sample was transferred onto the cryo-stage of an ALTO 2500 cryo-system (Gatan, Oxford, England) attached to an FEI Nova NanoSEM 450 field emission scanning electron microscope (SEM) (Thermo Fisher Scientific, Eindhoven, The Netherlands). Sublimation of surface frost was performed at $-95°C$ for 4 min before sputter coating with platinum for 150 s at 10 mA. The sample was moved onto the main cryo-stage in the microscope, held at $-125°C$, and imaged at 3 kV, spot 3, and digital TIFF files were stored.

Growth assays. To determine viability of *S. venezuelae* strains on solid medium, 10e5 CFU mL^{-1} (spores or mycelial fragments) were used to prepare a 10-fold serial dilution series, and 3 μL of each dilution series was subsequently spotted onto MYM agar containing either no antibiotic, 0.25 μg mL^{-1} MMC, 3 μg mL^{-1} ciprofloxacin, or 3 mM MMS. Plates, in biological triplicate, were incubated at 30°C for 3 to 5 days and subsequently imaged.

To assay the growth of *S. venezuelae* in liquid MYM, measurements of the optical density at 600 nm (OD_{600}) were made using a plate reader (SPECTROstar Nano by BMG Labtech) set at 30°C with shaking at 700 rpm. Eight hundred microliters of MYM supplemented with increasing concentrations of MMC, ciprofloxacin, or MMS was loaded into the wells of a 48-well plate (677102; Greiner Bio-One) and inoculated with either 5 μL of spores or 10 μL of mycelium. OD_{600} measurements were recorded every 15 min for 24 h, and data were subsequently visualized using GraphPad Prism (version 9.3.1). Each experiment was performed in triplicate.

Purification of His_6-LexA. To purify His_6-LexA, *E. coli* NiCo21(DE3) cells were transformed with the pLysS and pKS16 plasmids. Cells were grown at 30°C in LB medium containing 25 μg mL^{-1} chloramphenicol and 100 μg mL^{-1} carbenicillin until they reached an OD_{600} of 0.5, before the addition of 0.5 mM IPTG (isopropyl-β-D-1-thiogalactopyranoside) to induce protein production. Cultures were incubated with shaking at 30°C for 4 h and then harvested by centrifugation. Cell pellets were resuspended in a mixture of 50 mM Tris (pH 10.5), 1 M NaCl, and 10% glycerol with protease inhibitor (EDTA free; Merck) and lysed by sonication for 14 cycles at 18 microns amplitude with 15 s on and 10 s off. Lysates were centrifuged at 26,000 $\times$ *g* for 45 min at 4°C to remove cell debris and passed through a 0.45-μm-pore filter before being loaded on a HisTrap column via the ÄKTA pure system. (GE Healthcare). His_6-LexA was then eluted using an increasing concentration of imidazole. Fractions containing His_6-LexA were pooled and subjected to size exclusion chromatography on a HiLoad 16/600 Superdex 200-pg column (GE Healthcare) in a mixture of 50 mM Tris (pH 10.5), 200 mM NaCl, 10% glycerol, 0.5 mM dithiothreitol (DTT). The concentration of pooled protein fractions was determined by Bradford assay, and His_6-LexA was subsequently stored at $-80°C$ until further use. To produce antibodies against LexA from *Streptomyces*, His_6-LexA was overexpressed and purified as described above, and a total amount of 3.54 mg of purified protein was sent to Cambridge Research Biochemicals (United Kingdom) to be used to raise antibodies in rabbits.

Surface plasmon resonance. All surface plasmon resonance (SPR) experiments were performed using a Biacore 8K instrument (Cytiva). All measurements were performed with a single sensor chip SA (Cytiva), using the ReDCaT system, as described previously (64). Complementary single-stranded oligonucleotides containing the individual LexA binding sequences or a scrambled binding motif were annealed and subsequently diluted to a working concentration of 1 μM in HPS-EP+ buffer (0.01 M HEPES [pH 7.4], 0.15 M NaCl, 3 mM EDTA, 0.005% [vol/vol] surfactant P20). Each DNA was designed to contain the sequence of interest and a single-stranded extension on the reverse primer, which anneals to the ReDCaT sequence on the chip, enabling DNA of interest to be bound and stripped after each experiment. For each experiment double-stranded DNA (with a 20-base single-strand extension) was flowed over one flow cell on the chip at a flow rate of 10 μL min^{-1} for 60 s to allow annealing to the ReDCaT linker via the complementary DNA. Purified *S. venezuelae* His_6-LexA (diluted in HBS-EP+ buffer) was flowed over both the blank cell surface and the one containing the DNA to ensure the response seen was specific to binding to the DNA. To assess whether LexA bound the DNA, 1 μM and 0.5 μM His_6-LexA were used at a flow rate of 50 μL min^{-1} for 120 s before switching back to buffer flow to allow dissociation for 120 s. The DNA and any remaining protein were then removed with a wash over both flow cells at 10 μL min^{-1} with 1 M NaCl plus 50 mM NaOH. DNA sequences were tested in triplicate at two different protein concentrations, and the amount of binding was recorded as response units (RU).

To determine LexA binding kinetics, a single-cycle kinetics approach was used. DNA was initially captured as previously described on the test flow cell and then increasing concentrations of His_6-LexA (0.78125 nM, 1.5625 nM, 3.125 nM, 6.25 nM, 12.5 nM, and 25 nM) were injected over both the blank and DNA-bound flow cells at a flow rate of 100 μL min^{-1} for 120 s. At the end of all the His_6-LexA injections, HPS-EP+ buffer was flowed over the surface for 1,200 s to measure the dissociation. The DNA and any remaining bound protein were then removed using the wash with 1 M NaCl and 50 mM NaOH. The recorded sensorgrams were analyzed using Biacore Insight Evaluation software version 3.0.11.15423 (Cytiva). The following formulas were used to calculate R_{max} and $\%R_{max}$ values: R_{max} = (MW of LexA)/(MW of DNA) $\times$ RU $\times$ *n* $\times$ 0.78 and $\%R_{max}$ = (analyte binding RU)/R_{max} $\times$ 100. MW is the molar mass, RU is the DNA capture response, 0.78 is a constant used for estimating responses for DNA-protein interactions, and *n* is the binding stoichiometry. Raw data used to calculate R_{max} and $\%R_{max}$ are shown in Table S6. To calculate LexA binding kinetics, a fit was applied using a predefined kinetics 1-to-1 binding model provided with the Biacore 8K Evaluation Software 3.0.11.15423 (Cytiva). Data were plotted using GraphPad Prism (version 9.3.1).

Data availability. The authors confirm that all supporting data have been provided within the article or through supplementaly data files. Raw RNA-seq and ChIP-seq data have been deposited in the MIAME-

compliant ArrayExpress database (https://www.ebi.ac.uk/arrayexpress/) under accession no. E-MTAB-11556 and E-MTAB-11603.

SUPPLEMENTAL MATERIAL

Supplemental material is available online only.
SUPPLEMENTAL FILE 1, XLSX file, 0.1 MB.
SUPPLEMENTAL FILE 2, XLSX file, 0.03 MB.
SUPPLEMENTAL FILE 3, XLSX file, 0.2 MB.
SUPPLEMENTAL FILE 4, XLSX file, 0.04 MB.
SUPPLEMENTAL FILE 5, XLSX file, 0.02 MB.
SUPPLEMENTAL FILE 6, PDF file, 1.3 MB.

ACKNOWLEDGMENTS

REFERENCES

1. Radman M. 1975. SOS repair hypothesis: phenomenology of an inducible DNA repair which is accompanied by mutagenesis. Basic Life Sci 5A: 355–367. https://doi.org/10.1007/978-1-4684-2895-7_48.
2. Baharoglu Z, Mazel D. 2014. SOS, the formidable strategy of bacteria against aggressions. FEMS Microbiol Rev 38:1126–1145. https://doi.org/10.1111/1574-6976.12077.
3. Erill I, Campoy S, Barbé J. 2007. Aeons of distress: an evolutionary perspective on the bacterial SOS response. FEMS Microbiol Rev 31:637–656. https://doi.org/10.1111/j.1574-6976.2007.00082.x.
4. Burby PE, Simmons LA. 2020. Regulation of cell division in bacteria by monitoring genome integrity and DNA replication status. J Bacteriol 202: e00408-19. https://doi.org/10.1128/JB.00408-19.
5. Brent R. 1982. Regulation and autoregulation by lexA protein. Biochimie 64:565–569. https://doi.org/10.1016/s0300-9084(82)80088-6.
6. Hopwood DA. 2007. Streptomyces in nature and medicine: the antibiotic makers. Oxford University Press, Oxford, United Kingdom.
7. Bush MJ, Tschowri N, Schlimpert S, Flärdh K, Buttner MJ. 2015. c-di-GMP signalling and the regulation of developmental transitions in streptomycetes. Nat Rev Microbiol 13:749–760. https://doi.org/10.1038/nrmicro3546.
8. Huang T-W, Chen CW. 2006. A recA null mutation may be generated in Streptomyces coelicolor. J Bacteriol 188:6771–6779. https://doi.org/10.1128/JB.00951-06.
9. McAuley S, Huynh A, Howells A, Walpole C, Maxwell A, Nodwell JR. 2019. Discovery of a novel DNA gyrase-targeting antibiotic through the chemical perturbation of Streptomyces venezuelae sporulation. Cell Chem Biol 26:1274–1282.e4. https://doi.org/10.1016/j.chembiol.2019.06.002.
10. Gomez-Escribano JP, Holmes NA, Schlimpert S, Bibb MJ, Chandra G, Wilkinson B, Buttner MJ, Bibb MJ. 2021. Streptomyces venezuelae NRRL B-65442: genome sequence of a model strain used to study morphological differentiation in filamentous actinobacteria. J Ind Microbiol Biotechnol 48:kuab035. https://doi.org/10.1093/jimb/kuab035.
11. Bush MJ, Chandra G, Buttner MJ. 2021. Streptomyces venezuelae transcription start sites data. http://streptomyces.org.uk/vnz_tss.html. Accessed 13 June 2022.
12. Marteyn BS, Karimova G, Fenton AK, Gazi AD, West N, Touqui L, Prevost M-C, Betton J-M, Poyraz O, Ladant D, Gerdes K, Sansonetti PJ, Tang CM. 2014. ZapE is a novel cell division protein interacting with FtsZ and modulating the Z-ring dynamics. mBio 5:e00022-14. https://doi.org/10.1128/mBio.00022-14.
13. Hamoen LW, Haijema B, Bijlsma JJ, Venema G, Lovett CM. 2001. The Bacillus subtilis competence transcription factor, ComK, overrides LexA-imposed transcriptional inhibition without physically displacing LexA. J Biol Chem 276:42901–42907. https://doi.org/10.1074/jbc.M104407200.
14. Little JW, Mount DW, Yanisch-Perron CR. 1981. Purified lexA protein is a repressor of the recA and lexA genes. Proc Natl Acad Sci U S A 78:4199–4203. https://doi.org/10.1073/pnas.78.7.4199.

15. Brent R, Ptashne M. 1981. Mechanism of action of the lexA gene product. Proc Natl Acad Sci U S A 78:4204–4208. https://doi.org/10.1073/pnas.78.7.4204.
16. Bush MJ, Bibb MJ, Chandra G, Findlay KC, Buttner MJ. 2013. Genes required for aerial growth, cell division, and chromosome segregation are targets of WhiA before sporulation in Streptomyces venezuelae. mBio 4: e00684-13. https://doi.org/10.1128/mBio.00684-13.
17. Willemse J, Borst JW, de Waal E, Bisseling T, van Wezel GP. 2011. Positive control of cell division: FtsZ is recruited by SsgB during sporulation of Streptomyces. Genes Dev 25:89–99. https://doi.org/10.1101/gad.600211.
18. Ausmees N, Wahlstedt H, Bagchi S, Elliot MA, Buttner MJ, Flärdh K. 2007. SmeA, a small membrane protein with multiple functions in Streptomyces sporulation including targeting of a SpoIIIE/FtsK-like protein to cell division septa. Mol Microbiol 65:1458–1473. https://doi.org/10.1111/j.1365-2958.2007.05877.x.
19. Kelemen GH, Brian P, Flärdh K, Chamberlin L, Chater KF, Buttner MJ. 1998. Developmental regulation of transcription of whiE, a locus specifying the polyketide spore pigment in Streptomyces coelicolor A3(2). J Bacteriol 180:2515–2521. https://doi.org/10.1128/JB.180.9.2515-2521.1998.
20. Falguera JVT, Stratton KJ, Bush MJ, Jani C, Findlay KC, Schlimpert S, Nodwell JRY. 2022. DNA damage-induced block of sporulation in Streptomyces venezuelae involves downregulation of ssgB. Microbiology. https://doi.org/10.1099/mic.0.001198.
21. Bailey TL, Johnson J, Grant CE, Noble WS. 2015. The MEME Suite. Nucleic Acids Res 43:W39–W49. https://doi.org/10.1093/nar/gkv416.
22. Butala M, Klose D, Hodnik V, Rems A, Podlesek Z, Klare JP, Anderluh G, Busby SJW, Steinhoff H-J, Žgur-Bertok D. 2011. Interconversion between bound and free conformations of LexA orchestrates the bacterial SOS response. Nucleic Acids Res 39:6546–6557. https://doi.org/10.1093/nar/gkr265.
23. da Rocha RP, de Miranda Paquola AC, do Valle Marques M, Menck CFM, Galhardo RS. 2008. Characterization of the SOS regulon of Caulobacter crescentus. J Bacteriol 190:1209–1218. https://doi.org/10.1128/JB.01419-07.
24. Kawai Y, Moriya S, Ogasawara N. 2003. Identification of a protein, YneA, responsible for cell division suppression during the SOS response in Bacillus subtilis. Mol Microbiol 47:1113–1122. https://doi.org/10.1046/j.1365-2958.2003.03360.x.
25. Walter BM, Cartman ST, Minton NP, Butala M, Rupnik M. 2015. The SOS response master regulator LexA is associated with sporulation, motility and biofilm formation in Clostridium difficile. PLoS One 10:e0144763. https://doi.org/10.1371/journal.pone.0144763.
26. Huisman O, D'Ari R, Gottesman S. 1984. Cell-division control in Escherichia coli: specific induction of the SOS function SfiA protein is sufficient to block septation. Proc Natl Acad Sci U S A 81:4490–4494. https://doi.org/10.1073/pnas.81.14.4490.
27. Bibb MJ, Domonkos Á, Chandra G, Buttner MJ. 2012. Expression of the chaplin and rodlin hydrophobic sheath proteins in Streptomyces venezuelae is

controlled by σBldN and a cognate anti-sigma factor, RsbN. Mol Microbiol 84:1033–1049. https://doi.org/10.1111/j.1365-2958.2012.08070.x.

28. Michel B, Sandler SJ. 2017. Replication restart in bacteria. J Bacteriol 199: e00102-17. https://doi.org/10.1128/JB.00102-17.

29. Hoff G, Bertrand C, Piotrowski E, Thibessard A, Leblond P. 2018. Genome plasticity is governed by double strand break DNA repair in Streptomyces. Sci Rep 8:5272. https://doi.org/10.1038/s41598-018-23622-w.

30. Mukherjee A, Cao C, Lutkenhaus J. 1998. Inhibition of FtsZ polymerization by SulA, an inhibitor of septation in Escherichia coli. Proc Natl Acad Sci U S A 95:2885–2890. https://doi.org/10.1073/pnas.95.6.2885.

31. Masser EA, Burby PE, Hawkins WD, Gustafson BR, Lenhart JS, Simmons LA. 2021. DNA damage checkpoint activation affects peptidoglycan synthesis and late divisome components in Bacillus subtilis. Mol Microbiol 116: 707–722. https://doi.org/10.1111/mmi.14765.

32. Bojer MS, Wacnik K, Kjelgaard P, Gallay C, Bottomley AL, Cohn MT, Lindahl G, Frees D, Veening J, Foster SJ, Ingmer H. 2019. SosA inhibits cell division in Staphylococcus aureus in response to DNA damage. Mol Microbiol 112:1116–1130. https://doi.org/10.1111/mmi.14350.

33. Modell JW, Hopkins AC, Laub MT. 2011. A DNA damage checkpoint in Caulobacter crescentus inhibits cell division through a direct interaction with FtsW. Genes Dev 25:1328–1343. https://doi.org/10.1101/gad.2038911.

34. Szafran MJ, Gongerowska M, Małecki T, Elliot M, Jakimowicz D. 2019. Transcriptional response of Streptomyces coelicolor to rapid chromosome relaxation or long-term supercoiling imbalance. Front Microbiol 10:1605. https://doi.org/10.3389/fmicb.2019.01605.

35. Movahedzadeh F, Colston MJ, Davis EO. 1997. Determination of DNA sequences required for regulated Mycobacterium tuberculosis RecA expression in response to DNA-damaging agents suggests that two modes of regulation exist. J Bacteriol 179:3509–3518. https://doi.org/10.1128/jb.179.11.3509-3518.1997.

36. Vierling S, Weber T, Wohlleben W, Muth G. 2000. Transcriptional and mutational analyses of the Streptomyces lividans recX gene and its interference with RecA activity. J Bacteriol 182:4005–4011. https://doi.org/10.1128/JB.182.14.4005-4011.2000.

37. Cohn MT, Kjelgaard P, Frees D, Penadés JR, Ingmer H. 2011. Clp-dependent proteolysis of the LexA N-terminal domain in Staphylococcus aureus. Microbiology (Reading) 157:677–684. https://doi.org/10.1099/mic.0.043794-0.

38. Lovett CM, O'Gara TM, Woodruff JN. 1994. Analysis of the SOS inducing signal in Bacillus subtilis using Escherichia coli LexA as a probe. J Bacteriol 176:4914–4923. https://doi.org/10.1128/jb.176.16.4914-4923.1994.

39. Prasad D, Muniyappa K. 2020. The extended N-terminus of Mycobacterium smegmatis RecX potentiates its ability to antagonize RecA functions. Biochim Biophys Acta Proteins Proteom 1868:140468. https://doi.org/10.1016/j.bbapap.2020.140468.

40. Fudrini Olivencia B, Müller AU, Roschitzki B, Burger S, Weber-Ban E, Imkamp F. 2017. Mycobacterium smegmatis PafBC is involved in regulation of DNA damage response. Sci Rep 7:13987. https://doi.org/10.1038/s41598-017-14410-z.

41. Müller AU, Imkamp F, Weber-Ban E. 2018. The mycobacterial LexA/RecA-independent DNA damage response is controlled by PafBC and the Pup-proteasome system. Cell Rep 23:3551–3564. https://doi.org/10.1016/j.celrep.2018.05.073.

42. Gozzi K, Salinas R, Nguyen VD, Laub MT, Schumacher MA. 2022. ssDNA is an allosteric regulator of the C. crescentus SOS-independent DNA damage response transcription activator, DriD. Genes Dev 36:618–633. https://doi.org/10.1101/gad.349541.122.

43. Huang T-W, Hsu C-C, Yang H-Y, Chen CW. 2013. Topoisomerase IV is required for partitioning of circular chromosomes but not linear chromosomes in Streptomyces. Nucleic Acids Res 41:10403–10413. https://doi.org/10.1093/nar/gkt757.

44. Schmutz E, Hennig S, Li S-M, Heide L. 2004. Identification of a topoisomerase IV in actinobacteria: purification and characterization of ParYR and GyrBR from the coumermycin A1 producer Streptomyces rishiriensis DSM 40489. Microbiology (Reading) 150:641–647. https://doi.org/10.1099/mic.0.26867-0.

45. Munakata N, Rupert CS. 1972. Genetically controlled removal of "spore photoproduct" from deoxyribonucleic acid of ultraviolet-irradiated Bacillus subtilis spores. J Bacteriol 111:192–198. https://doi.org/10.1128/jb.111.1.192-198.1972.

46. Tapias A, Fernández S, Alonso JC, Barbé J. 2002. Rhodobacter sphaeroides LexA has dual activity: optimising and repressing recA gene transcription. Nucleic Acids Res 30:1539–1546. https://doi.org/10.1093/nar/30.7.1539.

47. Smollett KL, Smith KM, Kahramanoglou C, Arnvig KB, Buxton RS, Davis EO. 2012. Global analysis of the regulon of the transcriptional repressor LexA, a key component of SOS response in Mycobacterium tuberculosis. J Biol Chem 287:22004–22014. https://doi.org/10.1074/jbc.M112.357715.

48. Gutekunst K, Phunpruch S, Schwarz C, Schuchardt S, Schulz-Friedrich R, Appel J. 2005. LexA regulates the bidirectional hydrogenase in the cyanobacterium Synechocystis sp. PCC 6803 as a transcription activator. Mol Microbiol 58:810–823. https://doi.org/10.1111/j.1365-2958.2005.04867.x.

49. Jochmann N, Kurze A-K, Czaja LF, Brinkrolf K, Brune I, Hüser AT, Hansmeier N, Pühler A, Borovok I, Tauch A. 2009. Genetic makeup of the Corynebacterium glutamicum LexA regulon deduced from comparative transcriptomics and in vitro DNA band shift assays. Microbiology (Reading) 155:1459–1477. https://doi.org/10.1099/mic.0.025841-0.

50. Al-Bassam MM, Bibb MJ, Bush MJ, Chandra G, Buttner MJ. 2014. Response regulator heterodimer formation controls a key stage in Streptomyces development. PLoS Genet 10:e1004554. https://doi.org/10.1371/journal.pgen.1004554.

51. Gallagher KA, Schumacher MA, Bush MJ, Bibb MJ, Chandra G, Holmes NA, Zeng W, Henderson M, Zhang H, Findlay KC, Brennan RG, Buttner MJ. 2020. c-di-GMP arms an anti-σ to control progression of multicellular differentiation in Streptomyces. Mol Cell 77:586–599.e6. https://doi.org/10.1016/j.molcel.2019.11.006.

52. Culyba MJ, Kubiak JM, Mo CY, Goulian M, Kohli RM. 2018. Non-equilibrium repressor binding kinetics link DNA damage dose to transcriptional timing within the SOS gene network. PLoS Genet 14:e1007405. https://doi.org/10.1371/journal.pgen.1007405.

53. Courcelle J, Khodursky A, Peter B, Brown PO, Hanawalt PC. 2001. Comparative gene expression profiles following UV exposure in wild-type and SOS-deficient Escherichia coli. Genetics 158:41–64. https://doi.org/10.1093/genetics/158.1.41.

54. Jones EC, Uphoff S. 2021. Single-molecule imaging of LexA degradation in Escherichia coli elucidates regulatory mechanisms and heterogeneity of the SOS response. Nat Microbiol 6:981–990. https://doi.org/10.1038/s41564-021-00930-y.

55. Gust B, Challis GL, Fowler K, Kieser T, Chater KF. 2003. PCR-targeted Streptomyces gene replacement identifies a protein domain needed for biosynthesis of the sesquiterpene soil odor geosmin. Proc Natl Acad Sci U S A 100:1541–1546. https://doi.org/10.1073/pnas.0337542100.

56. Gust B, Chandra G, Jakimowicz D, Yuqing T, Bruton CJ, Chater KF. 2004. Lambda red-mediated genetic manipulation of antibiotic-producing Streptomyces. Adv Appl Microbiol 54:107–128. https://doi.org/10.1016/S0065-2164(04)54004-2.

57. Tschowri N, Schumacher MA, Schlimpert S, Chinnam N. b, Findlay KC, Brennan RG, Buttner MJ. 2014. Tetrameric c-di-GMP mediates effective transcription factor dimerization to control Streptomyces development. Cell 158:1136–1147. https://doi.org/10.1016/j.cell.2014.07.022.

58. Bush MJ, Chandra G, Al-Bassam MM, Findlay KC, Buttner MJ. 2019. BldC delays entry into development to produce a sustained period of vegetative growth in Streptomyces venezuelae. mBio 10:e02812-18. https://doi.org/10.1128/mBio.02812-18.

59. Langmead B, Salzberg SL. 2012. Fast gapped-read alignment with Bowtie 2. Nat Methods 9:357–359. https://doi.org/10.1038/nmeth.1923.

60. Li H, Handsaker B, Wysoker A, Fennell T, Ruan J, Homer N, Marth G, Abecasis G, Durbin R, 1000 Genome Project Data Processing Subgroup. 2009. The Sequence Alignment/Map format and SAMtools. Bioinformatics 25:2078–2079. https://doi.org/10.1093/bioinformatics/btp352.

61. Robinson MD, McCarthy DJ, Smyth GK. 2010. edgeR: a Bioconductor package for differential expression analysis of digital gene expression data. Bioinformatics 26:139–140. https://doi.org/10.1093/bioinformatics/btp616.

62. Kann MG, Sheetlin SL, Park Y, Bryant SH, Spouge JL. 2007. The identification of complete domains within protein sequences using accurate E-values for semi-global alignment. Nucleic Acids Res 35:4678–4685. https://doi.org/10.1093/nar/gkm414.

63. Schindelin J, Arganda-Carreras I, Frise E, Kaynig V, Longair M, Pietzsch T, Preibisch S, Rueden C, Saalfeld S, Schmid B, Tinevez J-Y, White DJ, Hartenstein V, Eliceiri K, Tomancak P, Cardona A. 2012. Fiji—an open source platform for biological image analysis. Nat Methods 9:676–682. https://doi.org/10.1038/nmeth.2019.

64. Stevenson CEM, Lawson DM. 2021. Analysis of protein-DNA interactions using surface plasmon resonance and a ReDCaT chip. Methods Mol Biol 2263:369–379. https://doi.org/10.1007/978-1-0716-1197-5_17.